Correlation of mechanical stress and Doppler broadening of the positron annihilation line in Al and Al alloys

C. Hugenschmidt,[1,*] N. Qi,[2] M. Stadlbauer,[1] and K. Schreckenbach[1]
[1]*Physics Department E 21 and FRM II, Technical University Munich, 85747 Garching, Germany*
[2]*Department of Physics, Wuhan University, Wuhan 430072, China*
(Received 8 October 2009; published 23 December 2009)

The plastic deformation of Al samples, of the technical alloys AlMgSi0.5, and AlMg3 was studied by Doppler-broadening spectroscopy (DBS) of the positron annihilation line. First, the defect sensitive line-shape parameter *S* was measured after the application of axial tensile stress, and the corresponding stress-strain curves were recorded that allowed us to correlate the strain, the mechanical stress and the *S*-parameter values after mechanical load quantitatively. In a next step, asymmetrically deformed Al samples were investigated with a monoenergetic positron beam by DBS in order to obtain the laterally resolved information of the stress-induced defects. It is demonstrated that the resulting two-dimensional *S*-parameter map (scan area 14×14 mm^2, step width 1 mm) can be expressed quantitatively in terms of the locally acting stress which is responsible for the creation of the lattice defects.

DOI: 10.1103/PhysRevB.80.224203 PACS number(s): 73.21.Ac, 78.70.Bj

I. INTRODUCTION

The characterization of the microstructure of technical materials during or after mechanical load plays an outstanding role in materials science and engineering applications. In order to improve the understanding of the material properties nondestructive techniques are crucial for the investigation of defects on the atomic scale, where the production of dislocations and vacancies is always interconnected during plastic deformation.[1,2] In addition, besides the detection of defects it is of great interest to apply methods for the visualization of plastically deformed areas in technical components.

There exist several techniques for the investigation of deformed materials: plastic deformation can be examined by ultrasonic or magnetic techniques where, however, e.g., tensile tests are required to calibrate the data (review of the methods can be found, e.g., in Ref. 3). The residual stress, which occurs for inelastic deformation, leads to local variations in the lattice spacing which can be investigated by neutron or x-ray diffraction. The measurement of the electrical resistivity is sensitive to all kind of defects but is not defect selective. Transmission electron microscopy, TEM, is particularly suited not only to visualize the lattice but also to determine the dislocation density. However, single vacancies and small vacancy clusters ($\leq$1 nm) cannot be detected. Positron annihilation spectroscopy (PAS), is well suited as a nondestructive technique, which is sensitive to dislocations and vacancies elastically bound to them. Moreover, the application of monoenergetic positron beams allows laterally resolved defect studies.

More than 40 years ago, Berko *et al.* demonstrated the sensitivity of positrons to defects in plastically deformed Al by the investigation of the angular correlation of the annihilation radiation.[4] In the following, it was shown by positron lifetime experiments, by Doppler-broadening (DBS) spectroscopy and by theoretical considerations that positron annihilation is, in particular, sensitive to dislocations and vacancies. Due to their binding energy of $E_b<100$ meV dislocation are shallow positron traps.[2,5–8] Dislocation lines are considered to act as precursor states for the transition into deeper traps, such as jogs[6,9] or vacancies, which are bound in the stress field around dislocations.[10,11] In molecular-dynamics studies on Al the positron binding energy was calculated to be 1.0 eV for a vacancy elastically bound to a dislocation line and 1.3 eV for a dislocation with a jog.[5] Since the formation of dislocations is accompanied by the production of vacancies associated to dislocations,[1,2,12] an enhanced positron trapping rate into these so-called *vacancylike* defects is observed. In particular, at large deformation and at fatigue, a high amount of vacancies is produced by the annihilation of edge dislocations.[13] The higher vacancy concentration along dislocation lines can be explained in terms of the vacancy formation energy which was calculated, e.g., for copper in the area around a dislocation line with the result that this energy is reduced to about 80% compared to the ideal lattice.[14]

In plastically deformed Al single crystals the increased positron lifetime was attributed to positron trapping in dislocations.[15] During tensile tests at polycrystalline Al, where positron trapping in dislocations and vacancylike defects was observed, the positron binding energy to dislocation lines was determined to $E_b=36$ meV by temperature-dependent PAS.[16] However, in positron lifetime experiments on plastically deformed samples only a mean lifetime for deformation-induced defects and the lifetime in the unperturbed lattice can be observed, and hence in most cases the type and the concentration of defects cannot be resolved.[17] In PAS on the Al alloys 2024 T3 and 7075 T6 no variation in the mean positron lifetime was observed during fatigue which was attributed to saturation positron trapping in precipitates.[18]

With the advent of positron microbeams[19] PAS with a spatial resolution in the submillimeter range became feasible, however, at the expense of beam intensity and hence longer measurement time. These experiments were performed by DBS (Refs. 20 and 21) or by positron lifetime measurements.[22] In the present work, the Doppler-broadening spectrometer at the high intensity positron beam

NEPOMUC was used allowing DBS with a spatial resolution of ≤ 300 μm within short measurement time of a few minutes.

In most DBS experiments the relative change in the rough line-shape parameter S (see Sec. II) is used to compare samples with various types and concentrations of defects after thermal or mechanical load or after irradiation. Thus, different defect types are usually not resolved because the S parameter is used to describe the average change in the microstructure.

The main goal of the present work is not only to scan the sample in two space dimensions but also to correlate the S parameter to a macroscopic entity such as strain or mechanical stress. For calibration purpose, stress-strain curves of several samples of Al and Al alloys were recorded, and the S parameter was determined for various strains after the tensile test. Then, plastically deformed asymmetrically shaped specimens were scanned with the monoenergetic positron beam in order to visualize the variation in the defect distribution in two dimensions after the mechanical load. Using the stress-strain and the S-strain data, the S parameter can be correlated with the mechanical stress which acted locally during the tensile test and hence was responsible for the creation of defects. By this procedure, we succeeded to image the local stress in the sample within a two-dimensional (2D) map.

II. POSITRON ANNIHILATION AND THE *S* PARAMETER

After implantation in a solid, the positron thermalizes very rapidly (few picoseconds) and annihilates with an electron by the emission predominantly of two collinear 511 keV γ quanta. In the experimental setups, a positron source or a monoenergetic positron beam with a state-of-the-art high-purity Ge detector is used for DBS. In the laboratory frame, the longitudinal projection of the electron momentum—the momentum of the thermalized positron can be neglected, onto the direction of the γ-ray emission p_L results in a Doppler shift of the 511 keV γ quanta by $\Delta E = \pm \frac{1}{2} p_L c$. Consequently, the detection of the Doppler-broadened 511 keV annihilation line enables a nondestructive examination of the electron momentum distribution at the positron annihilation site. In order to characterize changes in the annihilation line the line-shape parameter S was introduced which is defined by the ratio of the counts within a fixed interval of the central part of the line and the total counts of the annihilation line (see, e.g., in reviews on positron physics[23–25]). Low electron momenta would hence lead to a high S value.

When positrons are trapped in open-volume defects the annihilation probability with core electrons, which have a much higher momentum than valence electrons, is reduced. Therefore, compared to the ideal lattice, less annihilation events with high Doppler shifts of the annihilation radiation and a narrowing of the 511 keV annihilation line is observed that leads to a higher S parameter due to the locally reduced density of core electrons in vacancylike defects. Consequently, the S parameter in plastically deformed samples can be regarded as a measure for the amount of stress-induced defects such as dislocations and vacancylike defects.

III. MEASUREMENTS

A. Sample preparation

For the presented experiment, samples of the industrial Al alloys AlMgSi0.5 (3.3206) and AlMg3 (3.3535) as well as samples of pure Al ($\geq$99.99%) were prepared. The geometry of the specimens of the first set was adapted to the usual one applied for uniaxial tensile strain tests: the thickness of the specimens was 2 mm, at a length of 55 mm the cross section amounted to 10 mm^2, and the total length was 120 mm including the broader ends of 20 mm for mounting in the tensile apparatus. In addition, a second set of specimens out of Al and AlMg3 was prepared with a triangular-shaped notch (depth about 1–2 mm) for a tensile test in order to study the plastically deformed area around the notch. Before the tensile tests, all samples were annealed at 773 K in a vacuum of 4.2×10^{-6} mbar for 1 h. The tensile tests were carried out with a Zwick/Roell Z100 tensile apparatus. For the positron experiment, the central part of the samples was cut out at a length of 20 mm in order to fit in the sample holder. Before the DB measurements, all samples were cleaned with acetone and rinsed by deionized water.

B. Tensile tests

Uniaxial tensile tests until the elongation at fracture were performed at room temperature with several specimens of the Al and the Al alloys in order to record the stress-strain curves. For each material, a characteristic stress-strain curve with typical parameter settings of the tensile machine (preloading speed: 5 mm/min; testing speed: 2 mm/min) is shown in the Fig. 1. The length increase along the freely deformable length l of the sample between the grips is denoted by the strain $\epsilon = \Delta l / l$, and the mechanical stress $\sigma = F/A$ is the ratio of the force F acting along the axis of the sample with the cross-sectional area A. Two specimens with a notch made out of AlMg3 and Al, respectively, were stretched up to a local stress, where the formation of microcracks started at the notch tip (see images in Figs. 3 and 5).

C. DBS with monoenergetic positrons

The defects related to the plastically deformation are recorded spatially resolved with the use of a monoenergetic positron beam. For this purpose, the Doppler-broadening studies were carried out with the CDB spectrometer[26] located at the high intensity positron source NEPOMUC—neutron-induced positron source Munich.[27] The intensity of the 1 keV positron beam at the sample position was 2×10^6 moderated positrons per second. For all measurements, the sample potential was set to -25 kV according to a positron implantation energy of $E = 26$ keV which corresponds to a mean positron penetration depth of about 3.13 μm in Al. The total diameter of the 26 keV positron beam amounted to 1.6 mm. The measurement time was set to 450 s per point, leading to typically 8.5×10^5 counts in the 511 keV photo peak of a single spectrum. During the measurement, the 477.6 keV γ line of ^{7}Be was recorded in order to monitor the electronic stability and the energy resolution which was $\Delta E / E = 1.38/477.6$ keV.

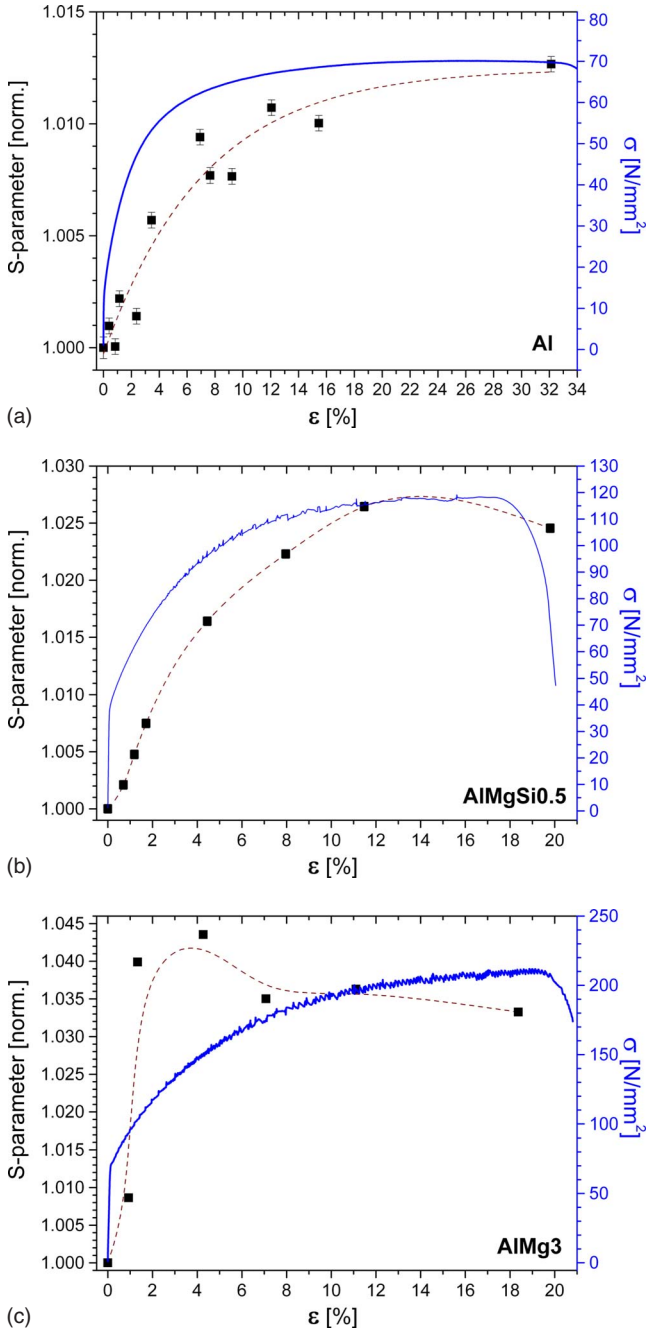

FIG. 1. (Color online) S parameter (left axis) after uniaxial strain tests normalized to $\epsilon=0$ and mechanical stress (right axis) as function of strain for pure Al, AlMgSi, and AlMg3. Dashed lines serve to guide the eye for the $S(\epsilon)$ curves.

First, the Doppler-broadened annihilation line was recorded after having differently elongated the samples of Al, AlMgSi0.5, and AlMg3. The obtained S-parameter values were normalized to the value of the untreated material and are plotted in Fig. 1 together with the stress-strain curves. Then, 2D scans of the asymmetrically deformed samples were performed with a step size of $\Delta x=\Delta y=1$ mm and the measurement time was set to 3 min per point. Hence, the total measurement time for a 2D scan amounted to about 3 and 13 h for AlMg3 and pure Al, respectively. The S parameter, which was normalized to the value of the untreated sample, is plotted as function of the space coordinates in Figs. 3 and 5.

IV. RESULTS AND DISCUSSION

A. Correlation of the S parameter, strain, and stress

Characteristic stress-strain curves were recorded for samples of Al, AlMgSi0.5, and AlMg3. Since uniaxial tensile tests are well reproducible only one representative curve for each material is plotted in Fig. 1.

Due the high ductility of annealed Al the elastic elongation at low stress is barely visible at Al whereas at the Al alloys, the linear elastic behavior according to Hook's law with the known Young's modulus of 70 kN/mm^2 is clearly visible at small strains of $\epsilon<0.2\%$. In comparison to the alloys the annealed Al sample is elongated to a much higher failing strain of about 34% which reflects the much higher ductility of pure annealed Al.

The starting points of the plastic deformation, and hence the nonlinear dependence of the stress σ, are at 37 and 62 N/mm^2 for AlMgSi0.5 and AlMg3, respectively. These values are lower than expected from the known $R_{p0.2}$ values for the tensile yield stress ($R_{p0.2}=160-230$ N/mm^2 for AlMgSi0.5 and $R_{p0.2}=80-140$ N/mm^2 for AlMg3). The obtained maximum stress is about 118 and 210 N/mm^2 for AlMgSi0.5 and AlMg3, respectively, which is also lower than the data from literature for the tensile strength ($R_m=215-260$ N/mm^2 for AlMgSi0.5 and $R_m=190-250$ N/mm^2 for AlMg3). This observation is explained by the difference of the tabulated values relevant for industrial as-received material and the measured values which are obtained by the uniaxial tensile test of annealed samples with accordingly low defect concentration at the beginning of the tensile test.

The measured S parameter as function of the strain ϵ shows a material specific behavior and, in particular, very different maximum values (see Fig. 1). The increase in the S parameter at low elongations demonstrates its high sensitivity to changes in the lattice if mechanical load is applied. For Al, the S parameter increases smoothly by about 1.25% to a maximum value at a strain of $\epsilon=32\%$. At AlMgSi0.5, similar to Al the S parameter rises with increasing ϵ but to a higher value. In contrast to Al or AlMgSi0.5, the alloy AlMg3 shows a steep S increase up to 1.04 already at low strains within $\epsilon<2\%$. Although the strain is low, a high stress of $\sigma>200$ N/mm^2 is required to elongate the AlMg3 sample further according to its higher hardness.

The observed S increase is attributed to the formation of dislocations and further growing dislocation density with higher strain. The accordingly high S parameter is explained by the creation of a high concentration of vacancylike defects such as jogs and vacancies during the tensile test. The tensile test with higher stress would also lead to residual stress, i.e., stress that remains locally in the sample after plastic deformation. Therefore, a higher S parameter would be expected due to the accordingly higher lattice spacing and hence a lower annihilation rate of core electrons which have higher momentum. However, residual stress is considered to be a tiny effect on S at highly deformed samples wherein the

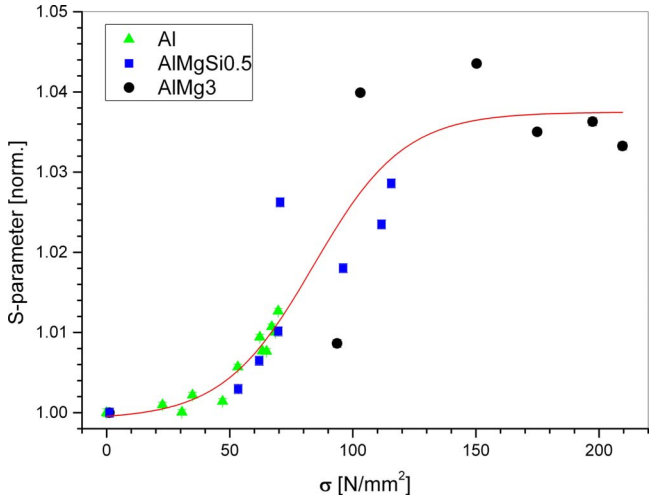

FIG. 2. (Color online) Correlation of the S parameter normalized to $\sigma=0$ and the mechanical stress for all samples obtained from Fig. 1. The solid line is a least-square fit of a sigmoidal curve to the experimental data.

presence of dislocations, jogs, (mono)vacancies attached at dislocations would act as efficient positron trapping sites.

For AlMgSi0.5 one observes a slight S decrease after the maximum stress of 118 $\mathrm{N/mm^2}$, and also for AlMg3 the S parameter at stresses between 180 and 210 $\mathrm{N/mm^2}$ is lower ($S \cong 1.035$) than the maximum value. This observation might be attributed to saturation trapping of positrons and related to the annihilation of vacancies due to the movement of dislocation during plastic deformation.

As observed for all materials the increasing S parameter to a maximum value is not directly correlated with the relative elongation ϵ of the samples. On the other hand, a more general correlation is observed between the S parameter and the stress σ. $S(\sigma)$ is plotted in Fig. 2 for all materials in order to demonstrate the relationship of the line-shape parameter S and the mechanical stress σ. The observed $S(\sigma)$ behavior is explained by the increasing defect density, i.e., increasing density of dislocations and vacancylike defects. Note that σ is not the residual stress but the mechanical stress during the tensile test which is responsible for the creation of defects.

The increase in S with higher defect concentration (single vacancies and divacancies) is well known from temperature-dependent DB measurements on Al.[28–30] Thermally induced defects lead to a rising S parameter with increasing temperature up to a certain temperature, where all positrons are trapped in vacancies or vacancy clusters, i.e., saturation trapping occurs.[28] The annihilation from different positron trapping sites such as dislocation lines, single vacancies or vacancy clusters would lead to small variations in the Doppler-broadened annihilation line. In a case study on Al results from *ab initio* calculations were compared with coincident DB spectra in order to distinguish between positrons trapped at thermally induced vacancies and vacancylike defects associated to dislocation lines.[31] It was shown in a recent DB study[32] on plastically deformed Al alloy AA2024 that the data analysis by using the W parameter provides no additional information to the S parameter which is in agreement to the observation of the present work.

In a previous study, temperature-dependent DBS in Al revealed a sensitivity limit of positrons to defects produced by plastic deformation that was found to be at a resolved shear stress of $\tau=4$ MPa, according to a dislocation density of about $2-3\times10^{12}$ $\mathrm{m^{-2}}$.[16] Results obtained on polycrystalline samples can be compared with those obtained on single crystals by using the relation between the axial flow stress σ and the shear flow stress τ acting at the primary glide plane of the dislocations $\tau=\sigma/M$, where $M=3.06$ denotes the so-called Taylor factor which accounts for multiple slip in the randomly oriented grains in the polycrystal. Hence, positrons became sensitive to plastic deformation at $\sigma=12$ $\mathrm{N/mm^2}$, and saturation trapping of positrons was not reached up to $\sigma=27$ $\mathrm{N/mm^2}$.[16] Both values agree with those of the present study (see Fig. 2).

In the present work, the measured $S(\sigma)$ data are approximated by a sigmoidal curve which is in good agreement with the S increase at low stress ($\sigma<70$ $\mathrm{N/mm^2}$). Even at higher σ, although the S values scatter largely, the curve still approximates the data as a plateau ($\sigma>150$ $\mathrm{N/mm^2}$), which can be attributed to saturation trapping of positrons. From the fitting routine it is obvious that more data is required for determining the saturation value and the correct functional slope of $S(\sigma)$ particularly at high stress more reliably.

In the following, the experimentally determined $S(\sigma)$ correlation is applied to serve as a quantitative measure for the stress σ during mechanical load. Consequently, the S values of plastically deformed samples, which were determined with a scanning positron beam in two dimensions, can be attributed to the mechanical stress, which was locally acting during mechanical load and hence was responsible for the creation of the lattice defects.

B. 2D scan of plastically deformed AlMg3

In the following measurement an AlMg3 sample with a notch was stretched up to a mechanical load, where tiny cracks at the notch tip became even visible by eye. Then two-dimensional DB measurements are performed in order to reveal open-volume defects in the neighborhood of the notch which were created during plastic deformation. Figure 3 shows the optical image and the S-parameter map of the AlMg3 sample with the notch after the tensile test. The color map clearly indicates the region of high S values according to the high mechanical stress that produced the lattice defects. As expected from the results for AlMg3 shown in Fig. 1, and also from the large scattering of the S at high σ in Fig. 2, it is barely possible to attribute single stress values to the measured S parameter. However, the largest fraction of the sample, shows a similar S parameter as AlMg3 samples which were stretched with a mechanical stress of $\sigma>150$ $\mathrm{N/mm^2}$.

C. 2D scan of plastically deformed Al

In contrast to AlMg3, the S parameter as function of σ shows a very smooth slope for the Al sample (see Fig. 4). The observed relationship between S and σ allows the correlation of the measured S parameter, which reflects a certain amount of different types of defects, to a certain mechanical

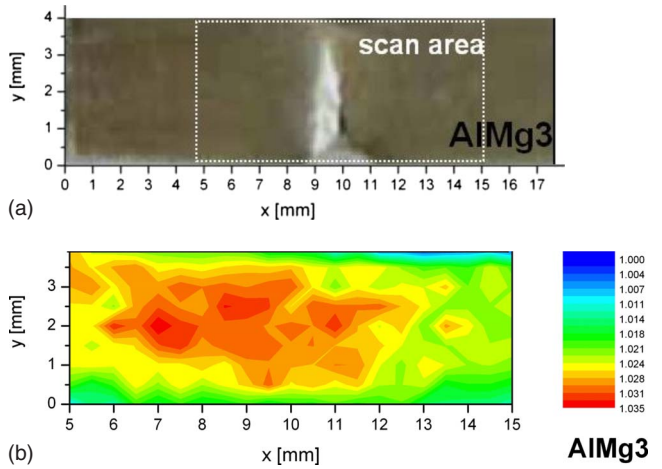

FIG. 3. (Color online) Asymmetrically deformed AlMg3 sample with a notch after tensile test: optical image (above), and 2D S parameter scan with a step width of 1 mm (below).

stress value in any mechanically treated Al sample. Hence, the measured S parameter of an, e.g., asymmetrically deformed Al sample can be interpreted in terms of the mechanical stress (see Sec. IV A).

Figure 5 shows an asymmetrical shaped Al sample with a notch after a tensile test. In the optical image the notch with a tiny crack is visible (Fig. 5 above). The resulting S parameter of the 2D positron scan of this sample is shown in (Fig. 5 below). For the interpretation of the data one can benefit from the $S(\sigma)$ relationship, which was visualized in Fig. 4. For this reason, the color legend of the spatially resolved $S(x,y)$ measurement can directly be converted into a stress map (see Fig. 5). It is emphasized that this plot is not a visualization of the residual stress but a map related to dislocations and vacancylike defects which are created at the same mechanical stress as observed in the tensile tests.

The area of largest deformation is clearly visible along the y direction of the crack propagation around $x=9$ mm. Due to the notch the cross section of the sample is reduced that leads

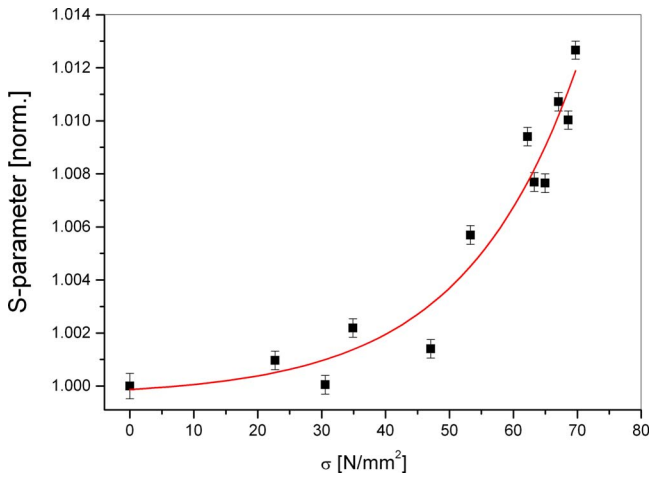

FIG. 4. (Color online) The S parameter normalized to $\sigma=0$ as function of the mechanical stress exclusively for the Al sample obtained from Fig. 1. The solid line is a least-square fit to the experimental data.

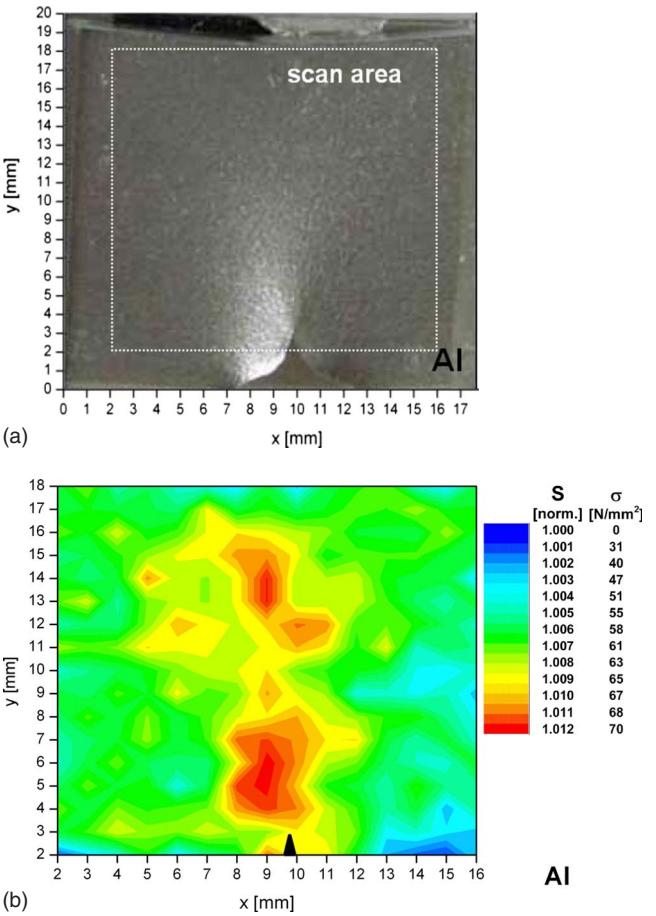

FIG. 5. (Color online) Asymmetrically deformed Al sample with a notch after tensile test: optical image (above), and 2D S-parameter scan with a step width of 1 mm leading to a stress map (below). Note the absolute values of the stress σ.

to a higher local stress in this region where the observed deformation corresponds to that one obtained at a stress of $\sigma > 67$ N/mm^2. At both sides of this central area, the S parameter decreases with increasing distance from the notch in x direction, which is attributed to a lower defect concentration. Hence, the stress decreases at both sides, and, e.g., at the green colored area the observed deformation can be attributed to the same defect density obtained for a sample which was stretched with $\sigma=55-63$ N/mm^2.

V. SUMMARY AND CONCLUSION

Conventionally, the rough line-shape parameter S obtained by DBS of the annihilation radiation is used to study open-volume defects in matter. Within the scope of the present work on Al, AlMgSi0.5, and AlMg3, we have demonstrated that DBS can be applied as powerful tool for the determination of the absolute value of the stress which was acting locally inside the sample during mechanical load. In addition, a monoenergetic positron beam was applied not only to scan the defect distribution in a nondestructive way but also to map the according local stress of plastically deformed samples.

Besides the specimens presented here, this technique could be used for various metals and technical alloys in order to determine the local stress after and during applied mechanical load. For this reason, it is planned to install an *in situ* tensile stress device inside the CDB spectrometer which will allow to collect about 25 DB spectra within 1 h. Currently, a new setup of the electrostatic lens system with a variable aperture is being mounted in order to improve the lateral resolution well below 100 μm within even lower measurement time.

ACKNOWLEDGMENTS

The authors thank M. Hölzel at the FRM II for providing the tensile test machine. The funding by the DAAD under Project No. A/05/16733 is gratefully acknowledged.

*christoph.hugenschmidt@frm2.tum.de; http://e21.frm2.tum.de/

[1] A. Seeger, Philos. Mag. **46**, 1194 (1955).
[2] P. B. Hirsch and D. H. Warrington, Philos. Mag. **6**, 735 (1961).
[3] G. Dobmann, N. Meyendorf, and E. Schneider, Nucl. Eng. Des. **171**, 95 (1997).
[4] S. Berko and J. C. Erskine, Phys. Rev. Lett. **19**, 307 (1967).
[5] H. Häkkinen, S. Mäkinen, and M. Manninen, Phys. Rev. B **41**, 12441 (1990).
[6] C. Hidalgo, G. González-Doncel, S. Linderoth, and J. San Juan, Phys. Rev. B **45**, 7017 (1992).
[7] E. Hashimoto, J. Phys. Soc. Jpn. **62**, 552 (1993).
[8] K. Petersen, I. A. Repin, and G. Trumpy, J. Phys.: Condens. Matter **8**, 2815 (1996).
[9] E. Hashimoto, M. Iwami, and Y. Ueda, J. Phys.: Condens. Matter **6**, 1611 (1994).
[10] V. M. Chernov, Phys. Status Solidi A **68**, 379 (1981).
[11] S. Mäkinen, S. Häkinen, and M. Manninen, Phys. Scr. T **T33**, 206 (1990).
[12] P. B. Hirsch, Philos. Mag. **7**, 67 (1962).
[13] U. Essmann and H. Mughrabi, Philos. Mag. A **40**, 731 (1979).
[14] J. Huang, M. Meyer, and V. Pontikis, Phys. Rev. Lett. **63**, 628 (1989).
[15] P. Hautojärvi, A. Tamminen, and P. Jauho, Phys. Rev. Lett. **24**, 459 (1970).
[16] T. Wider, K. Maier, and U. Holzwarth, Phys. Rev. B **60**, 179 (1999).
[17] T. Wider, S. Hansen, U. Holzwarth, and K. Maier, Phys. Rev. B **57**, 5126 (1998).
[18] U. Holzwarth and P. Schaaff, J. Mater. Sci. **42**, 5620 (2007).
[19] G. R. Brandes, K. F. Canter, and A. P. Mills, Phys. Rev. Lett. **61**, 492 (1988).
[20] H. Greif, M. Haaks, U. Holzwarth, U. Männig, M. Tongbhoyai, T. Wider, K. Maier, J. Bihr, and B. Huber, Appl. Phys. Lett. **71**, 2115 (1997).
[21] M. Maekawa and A. Kawasuso, Appl. Surf. Sci. **255**, 39 (2008).
[22] A. David, G. Kögel, P. Sperr, and W. Triftshäuser, Phys. Rev. Lett. **87**, 067402 (2001).
[23] R. N. West, Adv. Phys. **22**, 263 (1973).
[24] P. Schultz and K. Lynn, Rev. Mod. Phys. **60**, 701 (1988).
[25] P. Coleman, *Positron Beams and Their Applications* (World Scientific, Singapore, 2000).
[26] M. Stadlbauer, C. Hugenschmidt, B. Straßer, and K. Schreckenbach, Appl. Surf. Sci. **252**, 3269 (2006).
[27] C. Hugenschmidt, K. Schreckenbach, M. Stadlbauer, and B. Straßer, Nucl. Instrum. Methods Phys. Res. A **554**, 384 (2005).
[28] W. Triftshäuser, Phys. Rev. B **12**, 4634 (1975).
[29] K. Shizuma, E. Hashimoto, Y. Yoshizawa, and T. Kino, J. Phys. F: Met. Phys. **11**, 2461 (1981).
[30] M. J. Fluss, S. Berko, B. Chakraborty, P. Lippel, and R. W. Siegel, J. Phys. F: Met. Phys. **14**, 2855 (1984).
[31] A. Calloni, A. Dupasquier, R. Ferragut, P. Folegati, M. M. Iglesias, I. Makkonen, and M. J. Puska, Phys. Rev. B **72**, 054112 (2005).
[32] S. Hautakangas, H. Schut, S. van der Zwaag, P. R. D. del Castillo, and N. H. van Dijk, Phys. Status Solidi C **4**, 3469 (2007).